J Porous Mater (2018) 25:259–272
DOI 10.1007/s10934-017-0439-5

Evaluation of the effects of multiwalled carbon nanotubes on electrospun poly(3-hydroxybutirate) scaffold for tissue engineering applications

Moein Zarei[1] · **Saeed Karbasi**[2]

Published online: 9 May 2017

Abstract In this study, regarding the importance of optimal design and unique role of a scaffold in tissue regeneration and repair, poly(hydroxybutyrate) (PHB)/multiwalled carbon nanotubes (CNTs) nanocomposite scaffolds with different samples concentrations of CNTs (0, 0.5, 0.75, 1.0, and 1.25% w/v) was prepared by electrospinning technique. Morphological evaluation of scaffolds by using scanning electron microscopy showed the pore volume in all the scaffolds was over 80% and the addition of CNTs increased the average fiber diameter, from 210 nm (neat PHB) to 500 nm at 1.0% CNTs. To evaluate the structural properties of scaffolds, transmission electron microscopy and Fourier transform infrared spectroscopy were used and showed the presence of CNTs at along the fibers. The analysis of mechanical properties of the PHB/CNTs composites by using universal testing machine revealed great improvement over pure PHB scaffold, so that the tensile stress of the PHB/0.5%CNTs scaffolds was increased by 157%. The bioactivity of scaffolds was analyzed by placing them in simulated body fluid for 4 weeks and results showed that CNTs increase the bioactivity of scaffolds. The wettability of the scaffolds was evaluated with a conventional sessile drop method. The results of contact angles of surface showed that CNTs treatment increases the surface wettability. The attachment ability and viability of osteosarcoma cell lines MG-63 in presence of the scaffolds were also investigated. The attachment and proliferation of MG-63 were significantly increased in the PHB/CNTs scaffolds compared with the PHB control. Therefore, the PHB/CNTs composite scaffolds may be potentially useful in tissue engineering applications.

Keywords Scaffold · Poly(hydroxybutyrate) · Multiwalled carbon nanotubes · Electrospinning · Tissue engineering

1 Introduction

Tissue engineering began with the concept of using biomaterials and cells to assist the body in healing itself. As the discipline matured, its goal shifted to developing logical strategies for optimizing new tissue formation through the judicious selection of conditions that will enhance the performance of tissue progenitors in a graft site, ultimately encouraging the production of a desired tissue or organ. Several strategies are now available for developing new organs and tissues [1–6]. In this regard, three-dimensional porous scaffolds can be used with cells to provide many of the advantages of the methods described above. These preformed scaffolds are usually made of bioresorbable materials. The scaffolds promote new tissue formation by providing a surface and void volume that encourages attachment, migration, proliferation, and the desired differentiation of connective tissue progenitors throughout the region where new tissue is required [7–11].

Since the sizes of the majority of components of the extracellular matrix, such as porosities and the diameters of the fibers comprising them are at nano-scales, in recent

✉ Saeed Karbasi
Karbasi@med.mui.ac.ir

Moein Zarei
zarei.moein@yahoo.com

[1] Tissue Engineering Group, Faculty of Nuclear Engineering & Basic Sciences, Islamic Azad University, Najafabad Branch, Isfahan, Iran

[2] Department of Biomaterials and Tissue Engineering, School of Advanced Technology in Medicine, Isfahan University of Medical Sciences, Isfahan, Iran

years use of nano-fibers in tissue engineering has drawn a lot of attention [12–15]. Different techniques are available for the synthesis of nano-scale fibers of which the electrospinning technique is more important than others due to its controllability and low cost. Electrospinning is a process to synthesize nano-fibers and micro-fibers from polymer or composite solutions. One of the most important applications of this technique is the synthesis of three-dimensional scaffolds for use in tissue engineering [16, 17].

Different natural and synthetic materials have been used for the manufacture of three-dimensional scaffolds [18–21]. Of all the bio-environmental polymers, PHB, which has a long history of clinical uses such as tissue engineering applications, has undergone extensive research [22, 23]. This polymer which is synthesized by bacteria is polyester and is hydrolyzed in the human body to form butyric acid which is one of the metabolites of the body [24]. However, given the properties necessary for a scaffold, this polymer does not in itself have sufficient strength necessary for the synthesis of three-dimensional scaffolds [25]. Mechanically, nanoparticles of bioceramics play a critical role in providing mechanical stability. Iron et al. prepared a scaffold from PHB scaffold and bioactive glass nano-particles using the electrospinning technique [26]. Evaluation of the properties of the scaffold showed that the bioactive glass nano-particles improved the mechanical and bioactivity properties of the scaffold by the wt% of about ten [26].

Select the appropriate material to improve the mechanical and biological properties of PHB is important. Regarding this issue, carbon nanotubes exhibit many unique intrinsic physical, chemical and mechanical properties and have been intensively explored for biological and biomedical applications in the past few years [27, 28]. Many researchers have uncovered that properly functionalized CNTs are able to enter cells without toxicity, shuttling various biological molecular cargoes into cells [29]. However, despite those exciting findings, researchers have reported the negative sides of CNTs, showing that non-functionalized nanotubes are toxic to cells and animals [29]. CNT functionalization is thus required and involves the addition of functional groups such as carboxyl or alcohol groups to the walls and ends of the nanotubes. This should prevent CNT aggregation and allow for their incorporation into polymer scaffolds [30]. Biofunctionalization of CNTs surface with bioactive molecules, such as carbohydrates or peptides can help improve the biocompatibility and bioactivity of the scaffold. Once again their large surface area makes CNTs useful for tissue engineering purposes as large amounts of biomolecules can be placed onto the nanotubes [31].

CNTs without proper functionalization have a highly hydrophobic surface, and thus may aggregate in the cell culture and interact with cells by binding to various biological species including proteins via hydrophobic interactions, to induce certain cell responses such as cell toxicity [29]. Another important properly of CNTs is their strength and resistance, which is 100-fold of that of steel; but their specific gravity, is 1/6 times that of steel [32–34]. Jang et al. manufactured nano-composite scaffolds made of poly lactic glycolic acid and CNTs using the electrospinning technique [35]. The results showed a 54% increase in the strength of the scaffold in the presence of only 0.5% of multi-walled carbon nano-tubes. In another study, Yoo et al. add 1% of CNTs to polyvinyl alcohol scaffolds and reported an improvement in the mechanical properties of this scaffold [36]. Mechanically and biologically, nanoparticles of bioceramics can improve the properties of polymers. Researches have shown that, in order to enhance mechanical and biological properties of polymers by nanoparticles, have to a high amount of nanoparticles added to the basic polymer [37–41]. But In this context, a large number of other studies have shown that CNTs, with low percentages can significantly improve the properties of different polymers [42–44].

Regarding to effects of CNTs on the physical and mechanical properties of scaffolds, this study aims at preparing PHB/CNTs nanocomposite scaffolds by electrospinning and evaluating their surface morphology, fiber diameter distribution, mechanical properties, bioactivity, biocompatibility as well as the impact of CNTs content on the properties of these composite scaffolds for potential tissue engineering applications.

2 Experimental

2.1 Materials

The materials used were poly(3-hydroxybutirate) (Sigma-Aldrich Inc, USA), functionalized multi-walled carbon nano-tubes (COOH) measuring 5–25 nm in diameter, 0.5–2 μm in length and purity >95 wt% (Nanomaterials Pioneers Company, USA), dimethyl formamide (DMF) (MERCK, Germany), trichloromethane (TCM) (MERCK, Germany), simulated body fluid (SBF) (MERCK, Germany), Dulbecco's Modified Eagle's Medium (a-MEM) and trypsin (GIBCO Life Technologies, Grand Island, NY, USA), fetal bovine serum (FBS), MTT (M-2128, Sigma, St. Louis, MO, USA), dimethyl sulfoxide (DMSO), penicillin, and streptomycin.

2.2 Electrospinning of PHB/CNTs composite scaffolds

PHB/CNTs nanocomposite scaffolds were prepared by electrospinning. Briefly, PHB was dissolved in a mixture of TCM and DMF (7:3 v/v) at the concentration of 6% w/v. The functionalized CNT with five different sample

concentrations (0, 0.5, 0.75, 1.0, and 1.25% w/v) were added to the PHB solution and the mixture was ultrasonicated for 1 h. The electrospinning equipment used in the present study consisted of a 1 mL syringe, a needle with an internal diameter of 0.27 mm, an injection pump, an aluminum plate and a power source. The PHB/CNTs solution was loaded into the syringe with the needle attached. The needle was pointed toward the ground electrode and a constant positive voltage (12.5 kV) was applied to the needle. The distance between the needle tip and the ground electrode was 25 cm and the syringe pump, used to feed the polymer solution, was set at a flow rate of 0.01 mL/min. A fluid jet was formed from the needle and fibers were sprayed onto the aluminum foil to collect the fibers (Fig. 1). All experiments were carried out in air at 25 °C and 60% relative humidity.

2.3 Structural characterization of the scaffolds

The morphology of the surface of scaffolds was evaluated under a scanning electron microscope. The mean diameter of fibers was determined by measuring the diameters of 40 single fibers on the SEM photomicrograph. The porosity of the scaffolds, too, was investigated on the three SEM photomicrograph for each sample, using MATLAB software program. This method revealed that image analysis can easily be exerted to the porosity measurement of various layers [45]. Transmission electron microscopy (TEM) technique was used to evaluate the position and distribution pattern of CNTs within the fibers. FTIR technique was used to evaluate changes in the chemical structure of scaffolds.

2.4 Mechanical characterization of the scaffolds

Tensile strength test was used to evaluate the mechanical properties of scaffolds based on ISO 1798 specifications at room temperature [46]. The extension rate was kept at 10 mm/min and the load cell used was 20 N with a gauge length of 25 mm. The dimensions of the samples were10–50 mm (WL).

2.5 Surface wettability measurements

The majority of the measurements presented are of the static contact angle. The measurements of the contact angles were mainly made with the specimens placed in a horizontal plane using a telescope with a calibrated micrometer eyepiece. The contact angle measurements with a drop and to measure the angle 1 min after the deposition of the drop on the specimen [47]. On each occasion at least ten measurements were taken and the mean static contact angle was calculated using the Image J software.

2.6 Evaluation of bioactivity

Bioactivity of scaffolds nanocomposite by placement of scaffolds in SBF environment were analyzed for 4 weeks. For this purpose, AAS method (AAS-Perkin Elmer Co-A-Analyst-300) was used to determine the levels of calcium ions in the SBF solution after different sample immersion times. The analysis of presence and morphology of nanocomposite and observation of absorbed hydroxyapatite crystals on the surface of scaffolds was done with XRD and through SEM microscope (Mira 3-XMU).

2.7 MG-63 cells culture

The MG-63 cells derived from an osteosarcoma of a 14-year-old male (American Type Culture Collection, Rockville, MD, USA) were used in this study. The culture medium used was Dulbecco's modified Eagle's medium (DMEM) supplemented with 10% FBS and 1% penicillin/

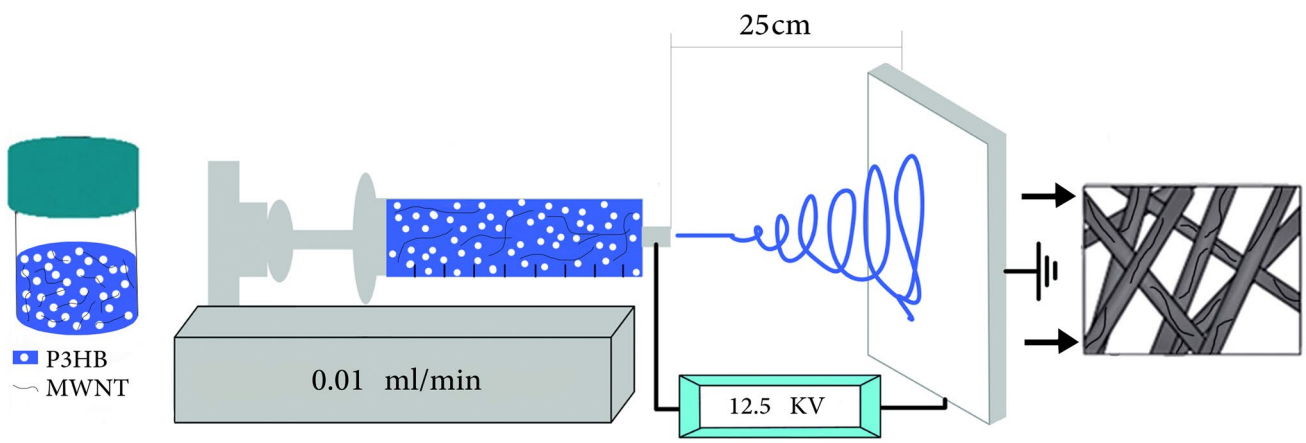

Fig. 1 The optimum electrospinning parameters for PHB/CNTs nanocomposite scaffolds

streptomycin. MG-63 cell lines were trypsinized using 0.1% trypsin and 0.1% ethylenediaminetetraacetic acid for 5 min, centrifuged at 400 g for 5 min, and resuspended in the medium. For determination of the cell adhesion and cell growth, the prepared scaffolds with 15 mm in diameter were placed in 24-welled tissue culture polystyrene plates (Corning, Action, MA, USA). A steel ring 15 mm diameter was placed on each of the tested scaffolds in the wells to prevent them from floating. Scaffolds and steel rings were sterilized in 70% ethanol overnight and rinsed extensively with phosphate-buffered saline (PBS), followed by treatment under ultraviolet light overnight. then, 1 mL of cell suspension in the concentration of 2×10^4 cells/mL was added to each well and maintained under standard cell culture conditions (humidified atmosphere, 5% CO_2/95% air environment, 37 °C). Cell suspension was also placed in empty tissue culture polystyrene dish with a steel ring as control groups.

2.8 Cell adhesion and proliferation

Cells adhering to the scaffolds were washed with PBS after 1 and 5 day incubation. Then, the cells were fixed with 2.5% glutaraldehyde in PBS at 4 °C for 1 h. The specimens, after being thoroughly washed with PBS, were dehydrated using graded ethanol changes, critical point dried; gold splattered in vacuum, and examined using SEM. After cell culturing for 1, 3 and 5 days, the viability of MG-63 cells was determined by MTT assay. MTT was prepared as a 5 mg/mL stock solution in PBS, sterilized by Millipore filtration (0.22 μm) and kept in dark. The 100 mL of MTT solution was added to each well. The MTT solution have incubated at 37 °C for 3 h, then 200 mL of dimethyl sulfoxide was added into each well to dissolve the formazan crystals. The dissolvable solution was jogged homogeneously about 15 min by the shaker. The optical density of the formazan solution was read on an ELISA plate reader at 570 nm. The analysis of variance (ANOVA) is used to determine whether there are any significant differences between the means of independent groups.

3 Results and discussion

3.1 Morphological characterization of composite scaffolds

Figure 2 presents the photomicrographs of pure PHB scaffold and PHB/CNTs nano-composite scaffolds with 0.5, 0.75, 1 and 1.25 wt%, with 20×30 mm dimensions. Pure PHB scaffold is completely white; however, the color of the fibers turned gray with an increase in the concentration of CNTs in the composite. It appears that the color centers of distinct scattering wavelengths are formed after the incorporation of different amounts of CNTs into the PHB matrix.

Figure 2 presents the SEM photomicrographs of pure PHB and PHB/CNTs nano-composite scaffolds. As shown in the figure, the synthesized fibers were mimetic of the natural extracellular matrix (ECM) which consists of fibers without any beads that are elongated and continuous and can serve as a basement membrane for cellular growth. The distributions of fiber diameters of pure PHB and PHB/CNTs scaffolds containing 0.5, 0.75, 1.0, and 1.25% CNTs are shown in Fig. 4. The diameter of the majority of fibers in pure PHB scaffolds was 180–320 nm, with a mean of 240 nm. The diameter of the composite fibers increased with increasing CNT content from 0.5 to 1.25% in the composites (this may be due to the viscosity effect) [48]. The addition of only 1% w/v CNTs resulted in a large increase in the diameter with the majority of fibers in the 400–590 nm range and an average diameter of 500 nm, which is about twice the diameter of the neat PHB fibers. Many studies have shown fiber diameter increased with the addition of second material [49]. The surface tension of the fluid emerging from the tip of the needle increased as the viscosity increased. This means under the same voltage, the elongation of the PHB/CNTs fibers was slower and that the jet stream reached the collector electrode before it split into thinner streams; thus thicker fibers were collected on the collector electrode. The phenomenon was

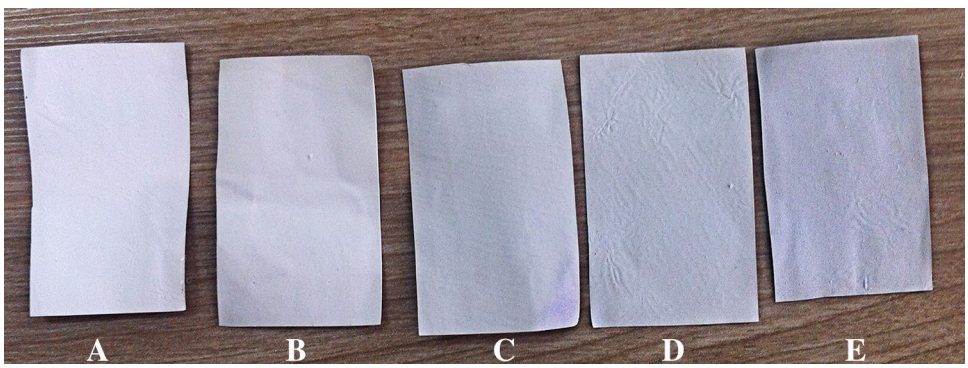

Fig. 2 The photographs of pure PHB scaffolds (*a*) and PHB/0.5% CNTs (*b*), PHB/0.75% CNTs (*c*), PHB/1% CNTs (*d*) and PHB/1.25% CNTs (*e*) scaffolds

common and it confirmed that viscosity is an important parameter during electrospinning [48]. With the addition of 1.25% CNTs, there was a broader distribution of fibers morphology that shown in Fig. 3. However, the CNTs tend to aggregate as the concentration is increased; thus the pinhole of the steel needle is easily blocked by the CNTs aggregates, which makes the electrospinning process difficult and the fiber distribution uneven.

3.2 Identification of the chemical structure

Changes in the chemical structure of the pure CNT powder, pure PHB scaffold and PHB/0.5%CNTs scaffold were examined by the FTIR machine (Fig. 5). In the spectrum obtained, vibrational modes were observed in 970–1725 cm^{-1} that indicates the structures and bonds of CH, CH_2, CH_3, C–O and O–H of PHB. In CNTs–COOH functionalized, characteristic vibrational modes of CNTs,

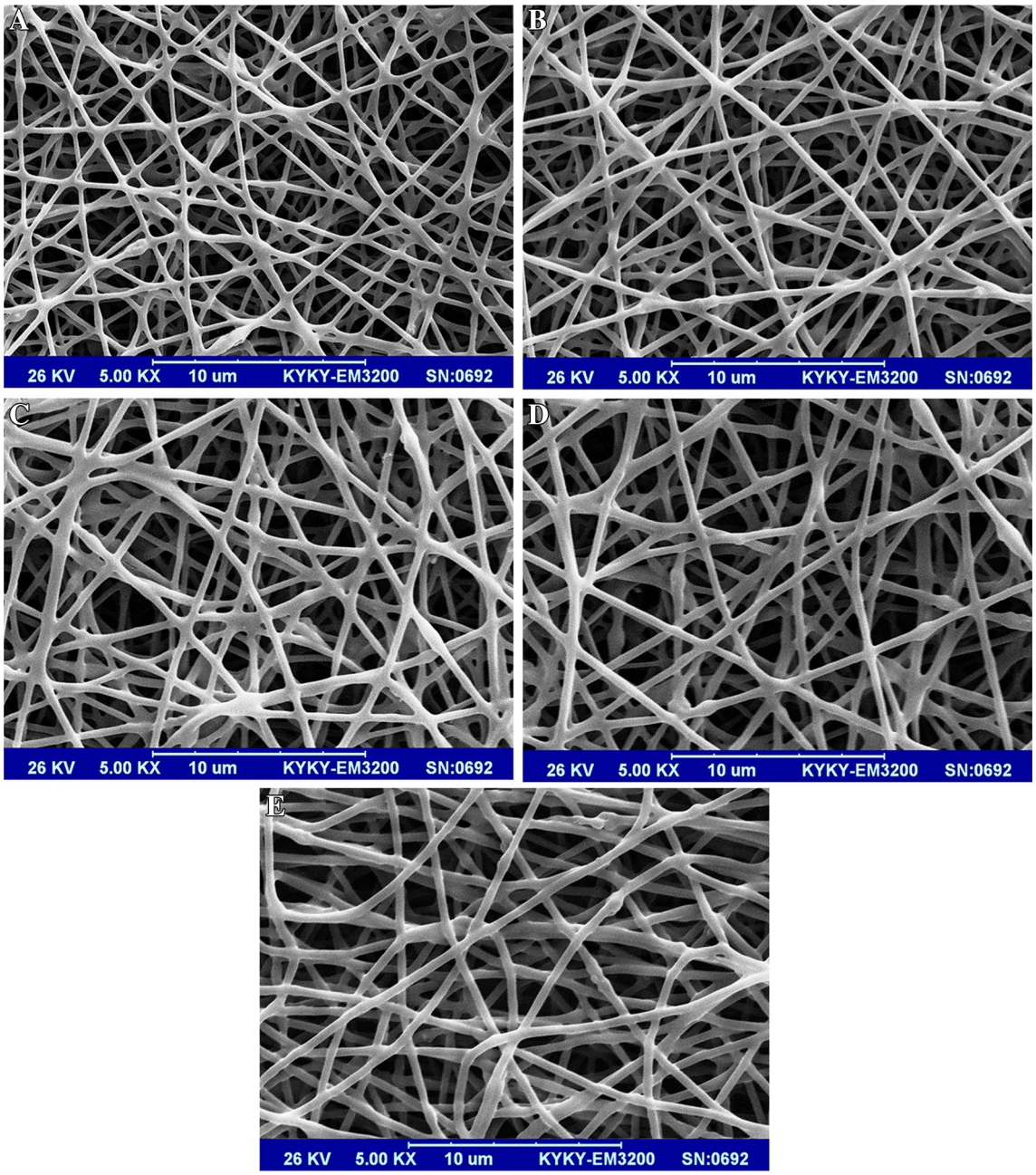

Fig. 3 SEM photomicrographs of pure PHB scaffolds (**a**) and PHB/0.5% CNTs (**b**), PHB/0.75% CNTs (**c**), PHB/1% CNTs (**d**) and PHB/1.25% CNTs (**e**) scaffolds

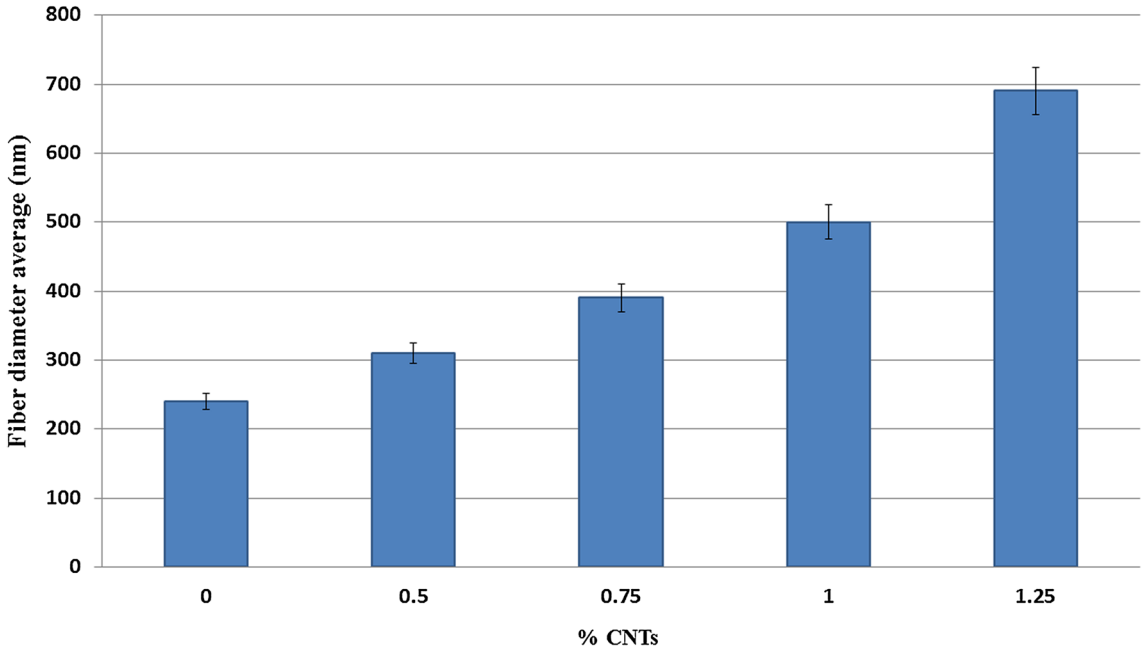

Fig. 4 An increase in the mean diameter of scaffold fibers proportional to the concentration of CNTs

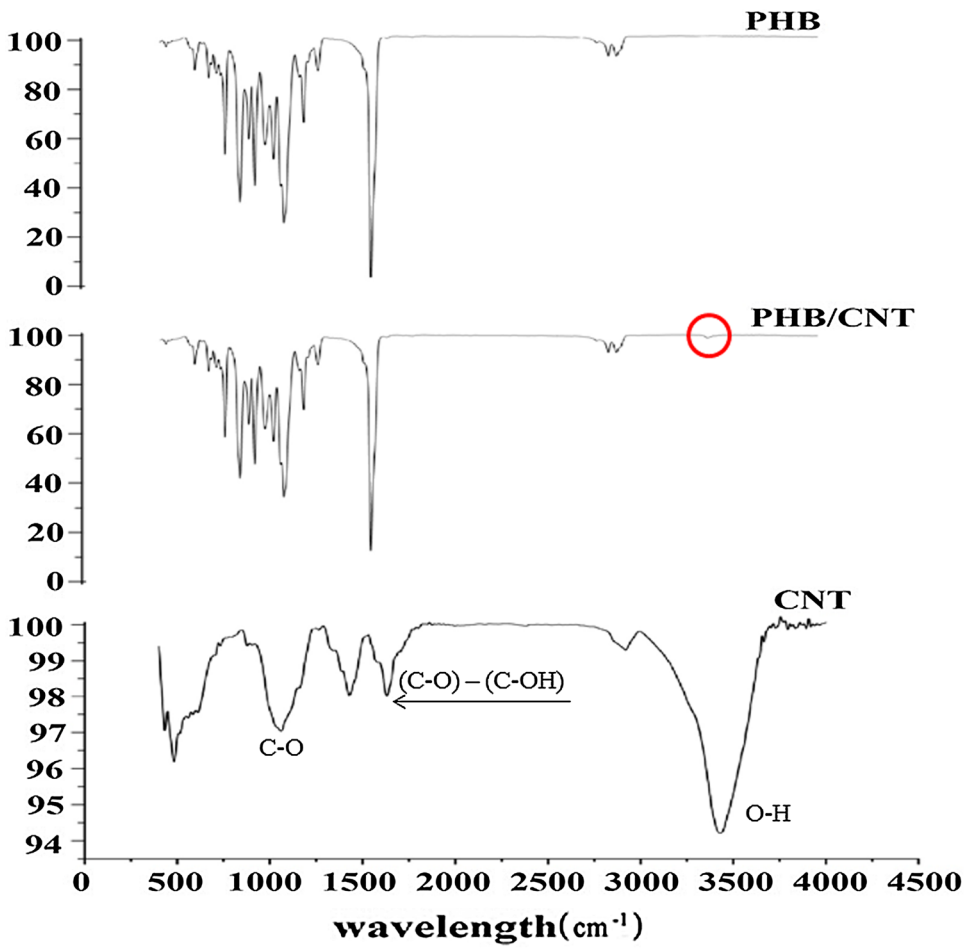

Fig. 5 FTIR of PHB, PHB/CNTs Nanocomposites and CNTs

C_C (1427–1630 cm^{-1}), O–H bonds (2910–3430 cm^{-1}) and C–O bond (870–1150 cm^{-1}) are apparent in the spectrum shown in Fig. 5. The electrospun PHB/CNTs nanocomposite scaffold spectrum, consist of nanotubes surface peak (O–H bond) at around 3430 cm^{-1}.

3.3 Morphology of CNTs in the structure of fibers

The TEM image of electrospun PHB/0.5%CNTs fibers is shown in Fig. 6. Nano-tubes are fine tubes that preserve their shape and most of them maintained their straight shape and are embedded within the fibers. A proper equilibrium has been achieved with the CNTs within the PHB fibers during the electrospinning process, in which CNTs are properly distributed and have been longitudinally oriented within the fibers.

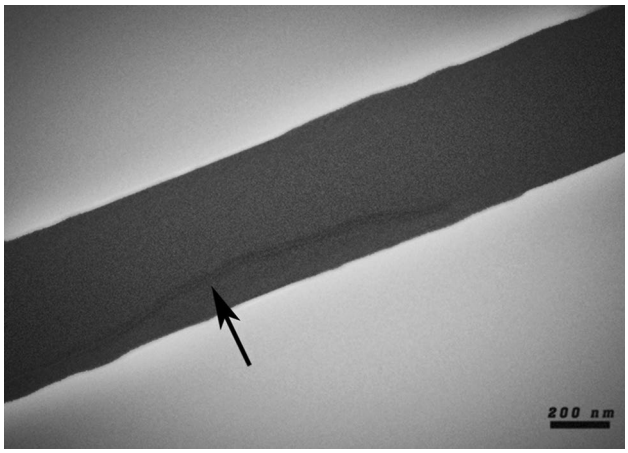

Fig. 6 TEM photomicrograph of PHB/0.5% CNTs nano-composite scaffold

3.4 Porosity of scaffolds

The only aspect of electrospinning that is not easy to directly control is the size of the scaffolds pores. This can be controlled indirectly by creating smaller diameter fibers, as smaller fibers result in smaller, more tightly packed pores [50, 51]. Stephen et al. characterized the dominant role of fiber diameter in controlling the pore diameter of the networks and reported that increasing fiber diameter results in an increase in mean pore radius [52]. However, it is not possible to alter pore size without changing any of the other electrospinning parameters [48]. The results of analyses carried out using MALAB software program in relation to the porosity of samples showed that the porosity rate in all the scaffolds was over 80%, which is favorable for tissue engineering purposes. Considering the porosity rates presented in Fig. 7, it seems the porosity increased from 82 to 85% with an increase in pore radius. The effects of fiber diameter and pore size on porosity characteristics were insignificant. Therefore, the CNTs have no negative effects in porosity of scaffolds.

3.5 Mechanical characterization

The tensile strengths of PHB scaffolds with different amounts of CNTs are shown in Fig. 8a. A plot of the variation in tensile modulus (MPa) as a function of CNTs content in the composites is in Fig. 8b. The role of CNTs in increasing the strength of nano-composite fibers is clearly evident. The highest strength was recorded in the PHB/0.5% CNTs, which increased by 157% (from 2 to 5.15 MP) in comparison to pure PHB scaffold and the Young's modulus increased by 163% (from 108 to 285 MP). The results indicated that CNTs can

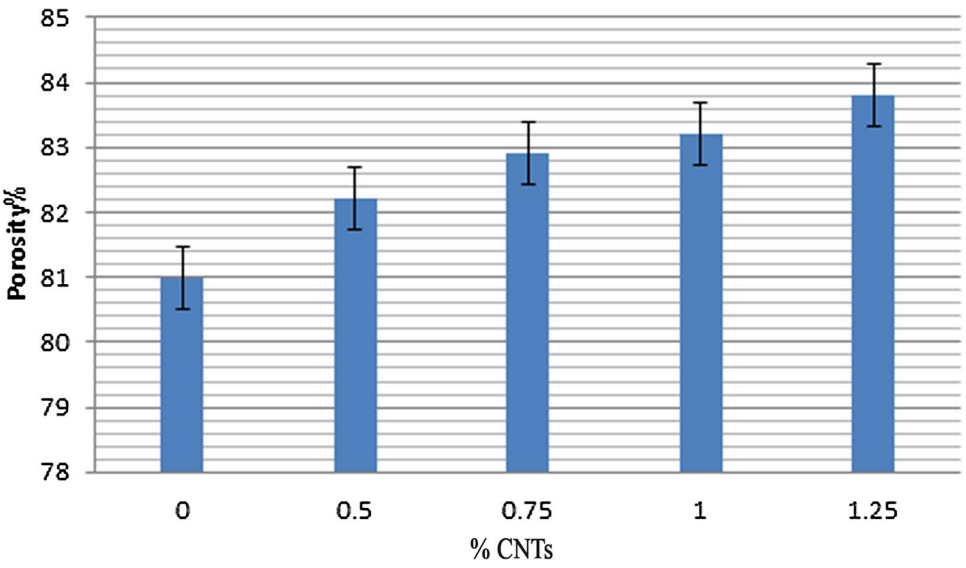

Fig. 7 Porosity rate of scaffolds in different amount of CNTs ($p < 0.05$)

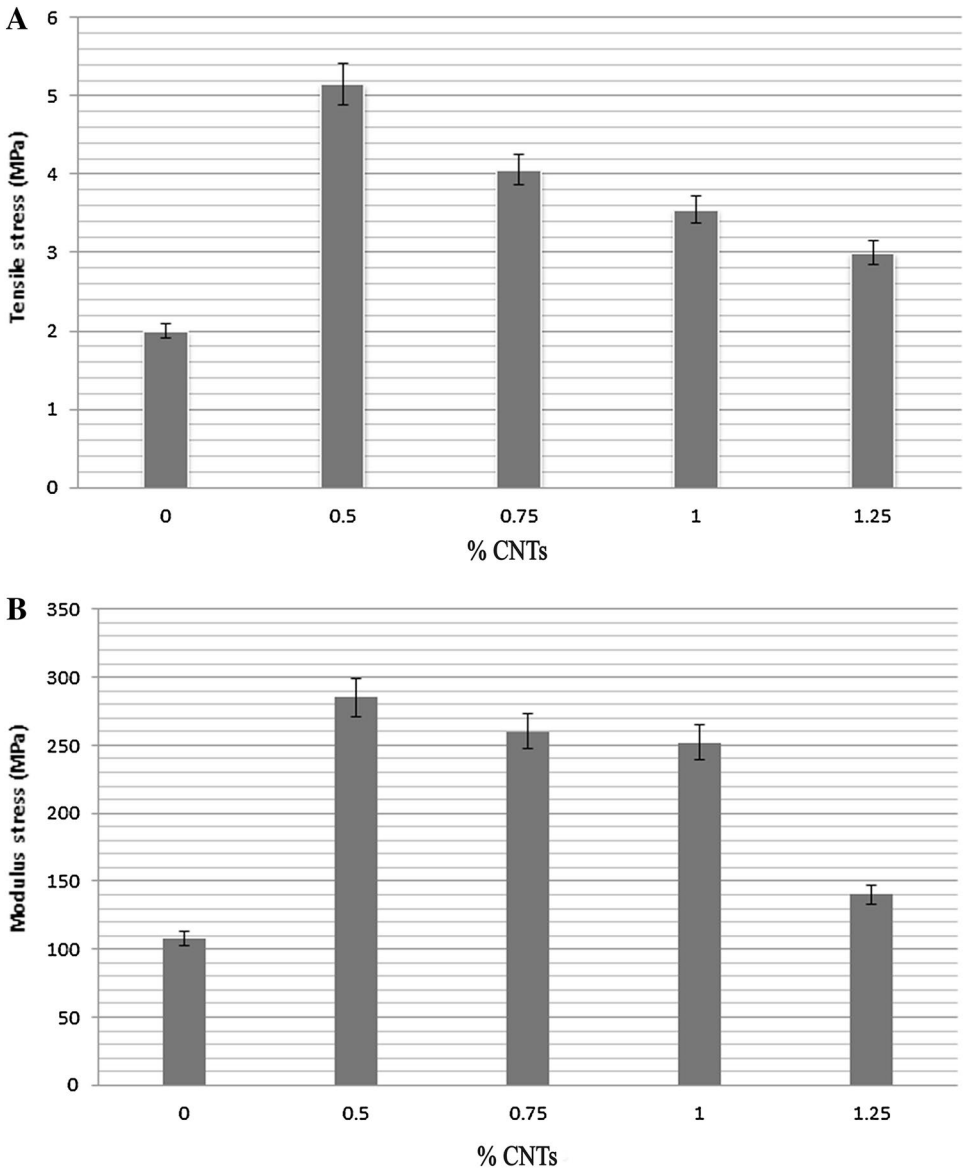

Fig. 8 **a** Changes in the tensile strengths of scaffolds in terms of changes in CNTs concentrations; **b** the modulus of scaffolds in terms of changes in CNTs concentrations

significantly increase the tensile strength and the modulus of nano-composite scaffold. In addition, the results showed the highest improvement in the mechanical properties of PHB/0.5% CNTs nano-composite scaffolds compared to pure PHB and other PHB/CNTs nano-composite scaffolds. Many studies have shown that a certain amount of CNTs increase the mechanical properties [48]. As mentioned, in order to enhance mechanical properties of polymers by nanoparticles, have to a high amount of nanoparticles added to the basic polymer [35–39]. Shor et al. added 25% of hydroxyapatite to poly(caprolactone) scaffold to increase the mechanical properties of scaffold [39]. Bagchi et al. by addition 20% wt of three different ceramic nanoparticles, namely, calcium titanate (CT), strontium titanate(ST) and barium titanate(BT), significantly increased the moduli and strength of poly(ε caprolactone) [41]. In this research, the low percentages of CNTs (only 0.5%) significantly improved the mechanical properties of PHB scaffold. the effect of the extent of the CNTs orientation on the modulus of the composite has been studied theoretically, by computing the deformation induced orientation of the CNTs and their Herman's orientation factor [36]. The initial increase in the tensile strength and tensile modulus (i.e. for the composites containing 0.5 wt% of filler) is attributed to the high degree of orientation of the filler CNTs in the wrapped nanofibers. As the wt% of filler in the nanofibers is further increased (i.e. 0.75, 1 and 1.25 wt%), agglomeration of the nanotubes takes place, which subsequently decreases their degree of anisotropy. Moreover, the agglomeration of the CNTs increases the weak van der Walls interaction between the CNTs bundles and the walls of the wrapped

nanofibers. However, these interactions are negligible at a lower wt% of CNTs, due to the directional anisotropy.

3.6 Water contact angle

Figure 9 shows the photos for a water drop of the on PHB and PHB/CNTs scaffolds. The wettability of scaffolds by water is increased by adding CNTs. Table 1 shows the contact angles for a water drop on the scaffolds after 1 min. The PHB scaffold presented a water contact angle (WCA) of 121° .Upon addition of 1.25% CNTs, the WCA decreases to 79°. Functional groups of CNTs (COOH) increased the amount of oxygen on the surface, increasing the quantity of C–O. This increment caused a significant reduction of WCA value in scaffolds [53].

Table 1 Static contact angle of water drops on scaffolds after 1 min

Contact angle	%CNTs
121°	0
97°	0.5
89°	0.75
86°	1
79°	1.25

3.7 Bioactivity test of the scaffolds

One of the signs of bioactivity is the ability to form apatite in SBF solution on the surface of PHB and PHB/CNTs scaffolds, which might occur in three ways.

Figures 10 and 11 show the SEM images and EDX of PHB and PHB/CNTs after bio adaptation test of samples in SBF solution. These images show the formation of apatite crystals on the surface of nanofibers after 28 days. As shown in the image, the relatively flat surfaces of fibers have become porous and irregular after submersion. Apatite particles were deposited widely with a brighter color compared to the surface of the fibers. Pure PHB scaffold showed least apatite particles compared to all other scaffold. This might have happened due to hydrophobic nature of PHB scaffold as determined by contact angle study. EDX results of the sample show the existence of calcium and phosphorus with a ratio of Ca/P = 1.6. It is clear that the results of EDX of the sample cannot be used to determine the exact chemical composition of the material. X-ray diffraction patterns were observed to determine the exact

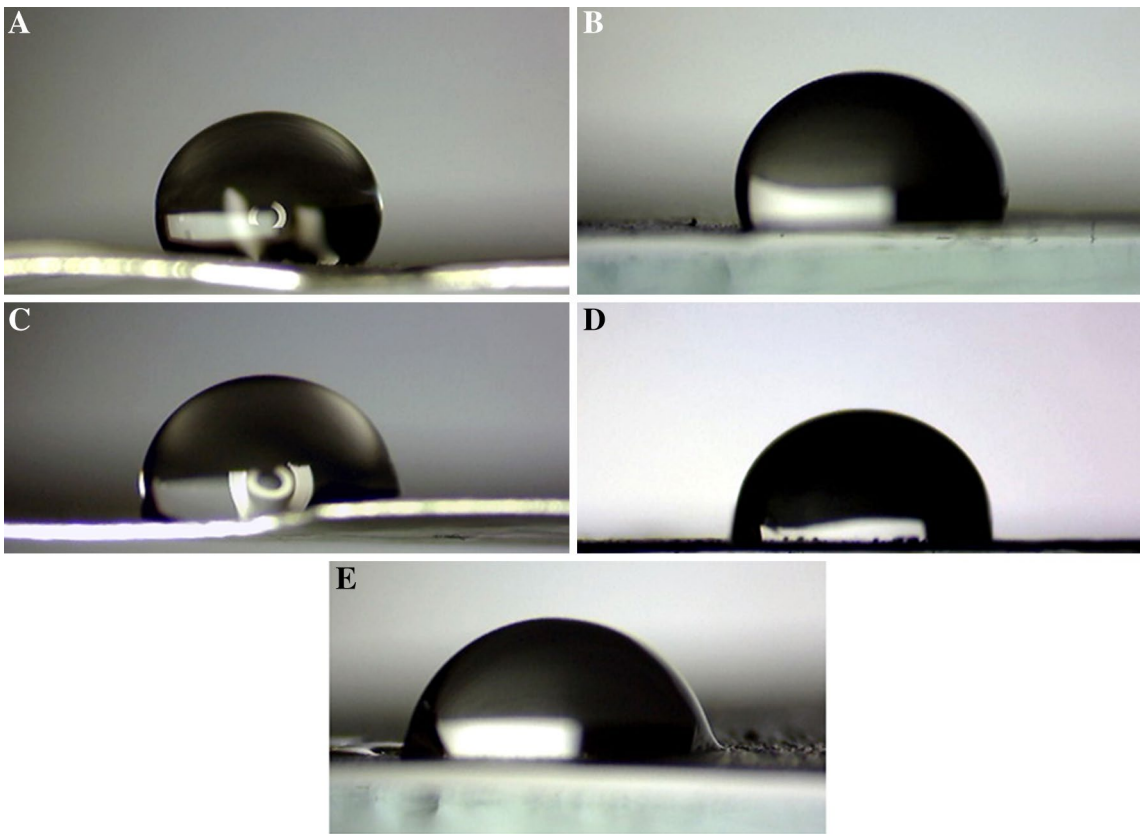

Fig. 9 Representative images of a 5 mL water droplet sitting over: pure PHB scaffolds (**a**), PHB/0.5% CNTs (**b**), PHB/0.75% CNTs (**c**), PHB/1% CNTs (**d**) and PHB/1.25% CNTs (**e**) scaffolds

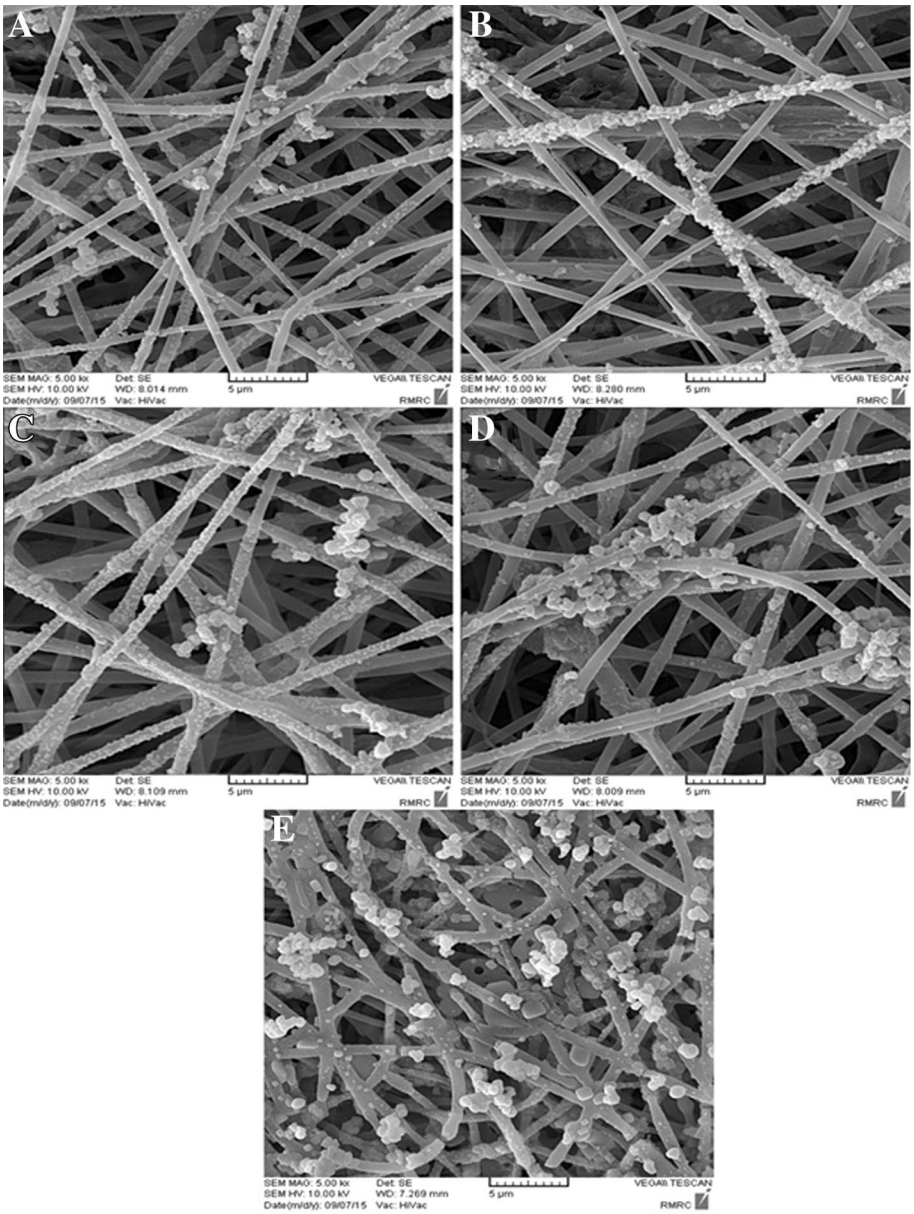

Fig. 10 SEM image of apatite particles constituent of pure PHB scaffolds (**a**), PHB/0.5% CNTs (**b**), PHB/0.75% CNTs (**c**), PHB/1% CNTs (**d**) and PHB/1.25% CNTs (**e**) scaffolds

chemical composition of the apatite particles on the surface of scaffolds.

The X-ray diffractogram of PHB/0.5%CNTs scaffolds before and after bioadaptation test of samples in SBF solution are shown in Fig. 12. As shown in the image the main peaks of HA phase is in the domain of 30°–35°.

An atomic percentage machine was used to study atomic absorption of calcium and its absorption percentage. In this method, after release of this element from the SBF solution, the level of calcium atomic absorption was defined, which showed less bioactive materials. A higher percentage of calcium in the solution indicated less absorption by the material, resulting in less bioactivity. To test atomic absorption, the concentration of calcium in SBF solution was measured, which was regarded as the control sample. The concentration of calcium in the control sample was 34 ppm (in Fig. 13). Then the concentration of calcium was registered on the 7th, 14th, 21th and 28th days. As shown in Fig. 13, on the 28th day, absorption of calcium ion by scaffolds were higher that show. Statistical analysis indicated that the absorption of calcium ion by PHB/CNTs scaffolds were higher than that of the PHB scaffolds. As a result, it can be concluded that CNTs within the scaffolds can increase bioactivity and formation of HA crystals on the surface of fibers.

3.8 MG-63 attachment on scaffolds

The adhesion and morphology of the cells on the scaffolds were observed after 24 h (fixed based on a preliminary

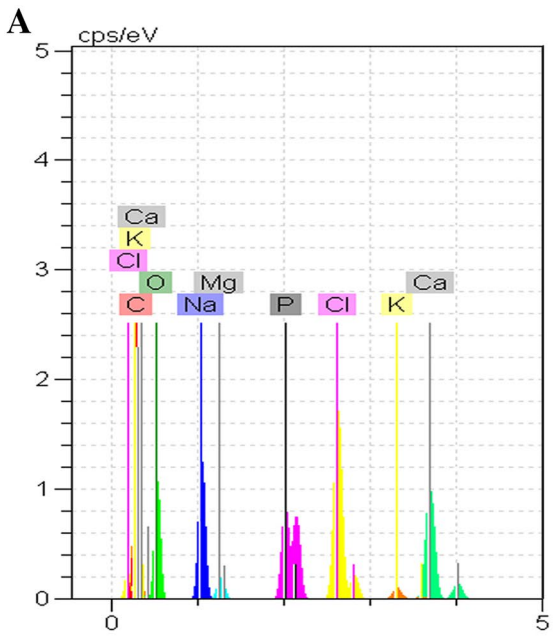

Element	Series	unn. C [wt.-%]	norm. C [wt.-%]	Atom. C [at.-%]
Carbon	K series	33.18	33.18	43.92
Oxygen	K series	45.50	45.50	45.22
Sodium	K series	1.21	1.21	0.83
Magnesium	K series	2.05	2.05	1.34
Silicon	K series	3.48	3.48	1.97
Phosphorus	K series	8.28	8.28	4.25
Chlorine	K series	0.78	0.78	0.35
Potassium	K series	0.48	0.48	0.19
Calcium	K series	4.37	4.37	1.73
Iron	K series	0.68	0.68	0.19
Total:		100.0 %		

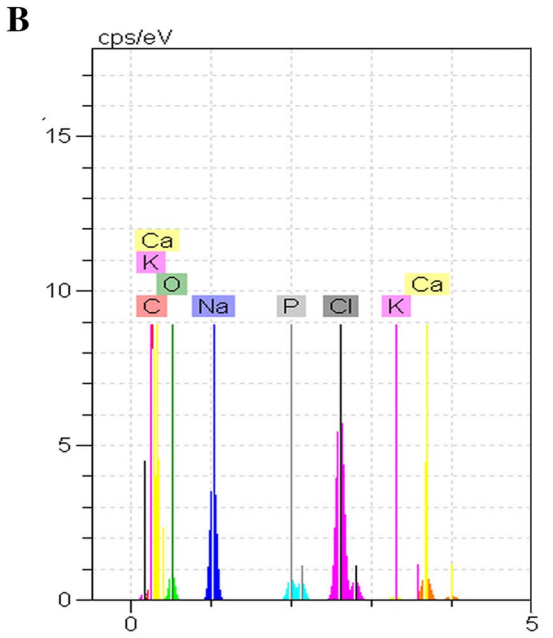

Element	Series	unn. C [wt.-%]	norm. C [wt.-%]	Atom. C [at.-%]
Carbon	K series	38.77	38.77	50.97
Oxygen	K series	40.20	40.20	39.68
Sodium	K series	0.45	0.45	0.31
Phosphorus	K series	7.55	7.55	3.85
Chlorine	K series	1.05	1.05	0.47
Calcium	K series	11.99	11.99	4.72
Total:		100.0 %		

Fig. 11 EDX analysis of pure PHB scaffolds (**a**) and PHB/1% CNTs (**b**) after 28 day in SBF Solution

study for optimum cell attachment) of cell seeding, the scaffolds were air dried and observed under SEM (Fig. 14). SEM micrographs showed that the cells attached firmly on all scaffolds. PHB scaffold showed least number of cells adhered compared to all other scaffold. This might have happened due to hydrophobic nature of PHB scaffold too (as determined by contact angle study). Hydrophobic surfaces exhibit poor cell adhesion [54]. Compared to the pure PHB scaffolds, cells on the PHB/CNTs composites were spread more. The cells had better adhesion on the PHB/1.25%CNTs scaffolds.

3.9 MTT assay

The response and cytotoxicity of various PHB/CNTs scaffolds on MG-63 was investigated by the MTT assay for 5 days. The MG-63 proliferation cultured on the PHB/CNTs composite scaffolds and on the empty tissue culture

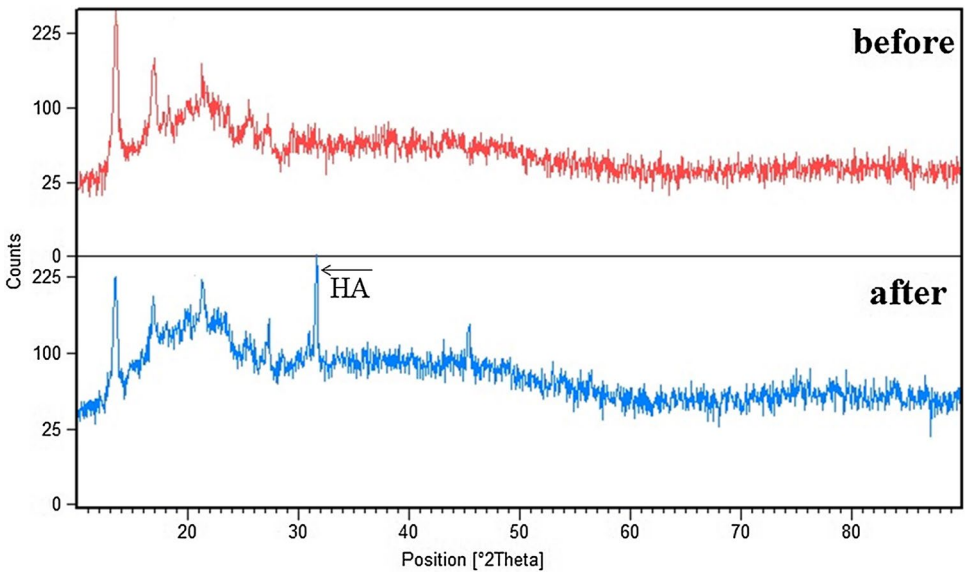

Fig. 12 XRD of PHB/1%CNTs (*before* and *after* submersion in SBF solution)

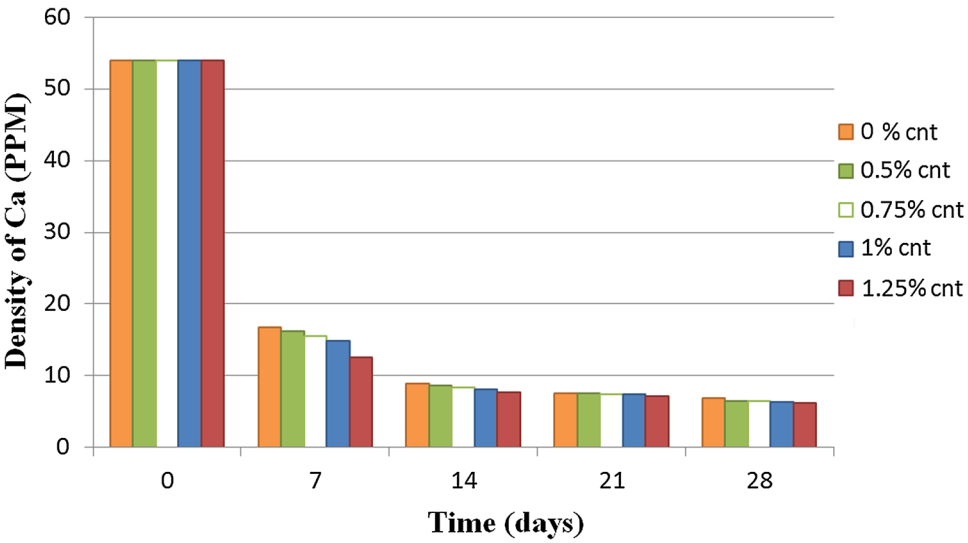

Fig. 13 Absorption of Calcium Ione of SBF solution by scaffolds in 7th, 14th, 21th and 28th days

polystyrene dish with a steel ring as control groups were evaluated. Figure 15 clearly indicates that the scaffolds did not have any toxic effect on the MG-63 cells. The presence of CNTs in scaffolds increased the viability of cells. However, After 5 days of culture, the percentage viability of the cells on the scaffolds containing 0.5, 0.75, 1.0, and 1.25% CNTs all significantly increased compared to the pure PHB scaffold ($p < 0.05$). Based on the in vitro data, these PHB/CNTs composite fibrous scaffolds offer favorable adhesion and growth of MG-63s. Since scaffolds act as a substrate for cellular attachment, proliferation, and differentiation, research efforts are focused on inducing the cells, to migrate into scaffolds and to proliferate and differentiate more effectively. In this context, CNTs could enhance the functions of osteoblasts (specifically, proliferation, differentiation, synthesis of alkaline phosphatase, and concentration of calcium in the extracellular matrix) [35].

4 Conclusions

PHB/CNTs scaffolds were successfully fabricated by electrospinning that mimicked the structure of a natural ECM. TEM and FTIR observations confirmed that most CNTs distributed uniformly within the fibers. The mechanical properties of the PHB/CNTs composites were greatly improved compared to the pure PHB scaffold. CNTs could improve the wettability, bioactivity and cell ability of the scaffolds and could potentially be used in tissue regeneration.

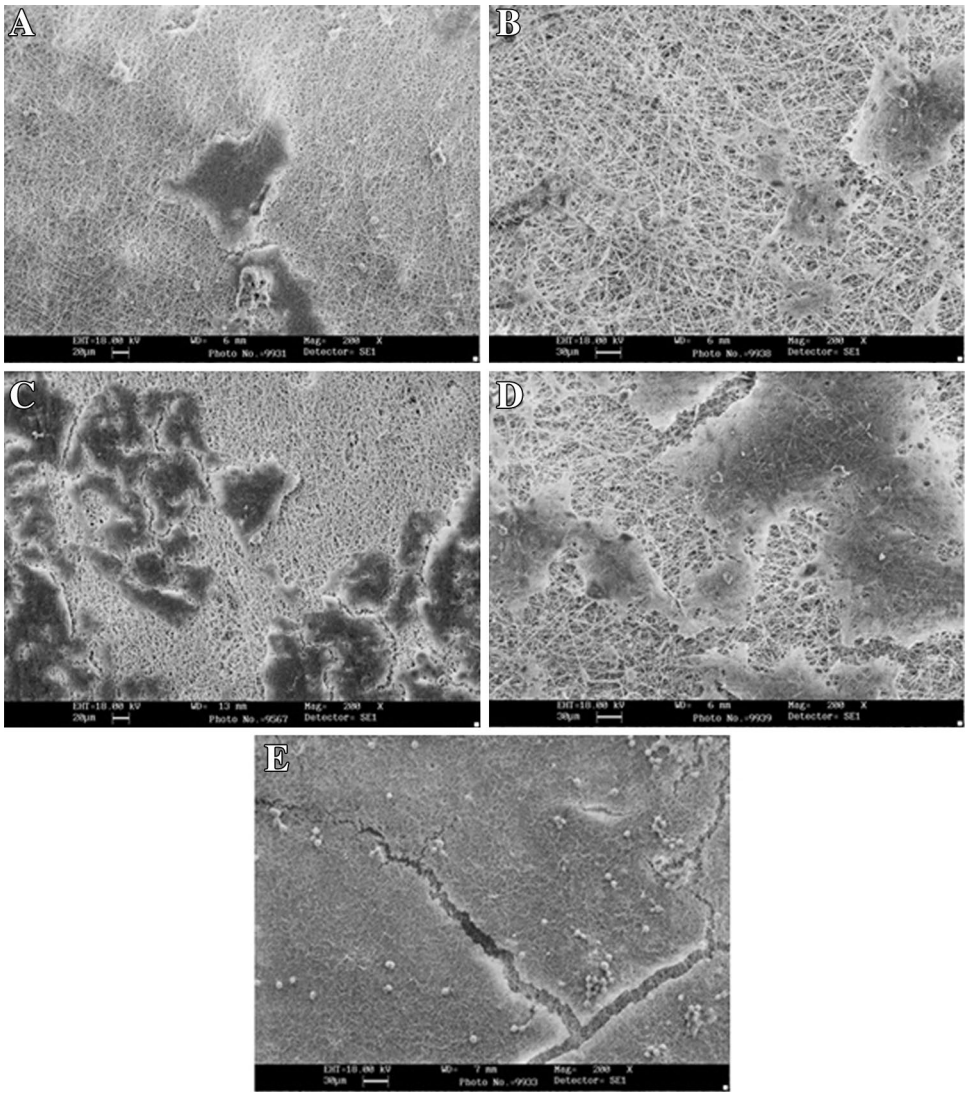

Fig. 14 SEM images of cell morphology on pure PHB scaffolds (**a**), PHB/0.5% CNTs (**b**), PHB/0.75% CNTs (**c**), PHB/1% CNTs (**d**) and PHB/1.25% CNTs (**e**) scaffolds

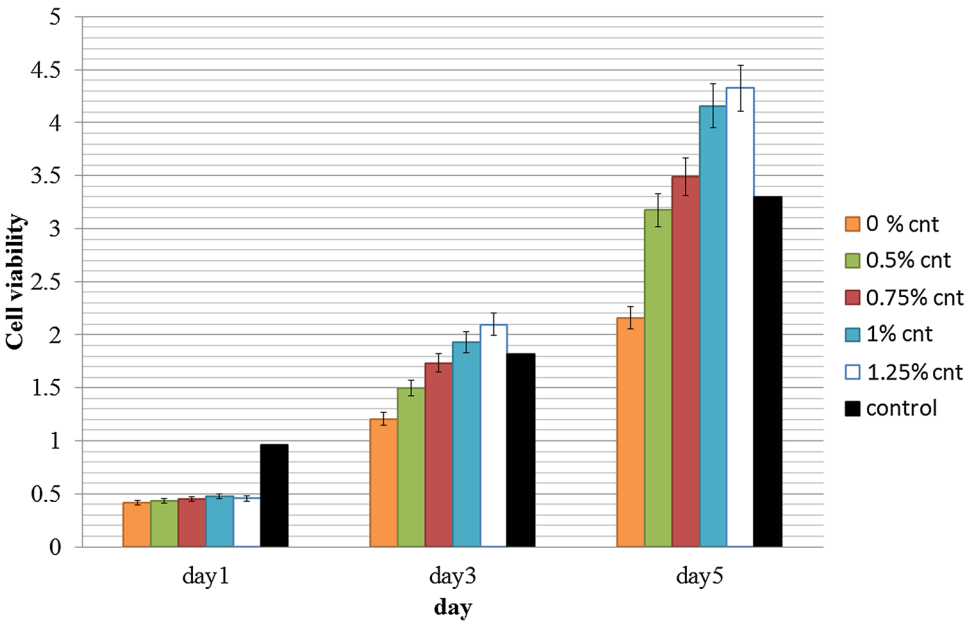

Fig. 15 Proliferation of MG-63 cells on the electrospun PHB, PHB/0.5%CNTs, PHB/0.75%CNTs, PHB/1%CNTs and PHB/1.25%CNTs scaffolds evaluated by MTT test at 1, 3, and 5 days. *Bar* represents mean ± SD. $p < 0.05$, one-way ANOVA test

References

1. H. Abukawa, H. Terai, D. Hannouche, J.P. Vacanti, L.B. Kaban, M.J. Troulis, J. Oral. Maxillofac. Surg. **61**, 94 (2003)
2. D.J. Aframian, R. David, H. Ben-Bassat, E. Shai, D. Deutsch et al., Tissue Eng. **10**, 914 (2004)
3. E. Alsberg, E.E. Hill, D.J. Mooney, Crit. Rev. Oral. Biol. Med. **12**(1), 64 (2001)
4. F.A. Auger, F. Berthod, V. Moulin et al., Biotechnol. Appl. Biochem. **39**(Pt 3), 263 (2004)
5. P.M. Bartold, C.A. McCulloch, A.S. Narayanan et al., Periodontology **24**, 253 (2000)
6. B.J. Baum, D.J. Mooney, J. Am. Dent. Assoc. **131**, 309 (2000)
7. C.M. Agrawal, R.B. Ray, J. Biomed. Mater. Res. **55**, 141 (2001)
8. L. Almany, D. Seliktar, Biomaterials **26**, 2467 (2005)
9. G.H. Altman, F. Diaz, C. Jakuba et al., Silk-based biomaterials. Biomaterials **24**, 401–416 (2003)
10. S.F. Badylak, Transpl. Immunol. **12**, 367 (2004)
11. L.R. Sakaguchi, J.M. Powers, in *Craig's Restorative Dental Materials*, 13th edn. Tissue engineering (Elsevier Mosby, St. Louis, MO, 2015), pp. 369–384
12. A. Hasan, A. Memic, N. Annabi, M. Hossain, A. Paul, R. Mehmet, F. Dehghani, A. Khademhosseini, Acta Biomater. **10**(1), 11 (2013)
13. J. KucinskaLipka, I. Gubanska, H. Janik, M. Sienkiewicz, Mater. Sci. Eng. C. **46**, 166 (2015)
14. T. Jiang, J.E. Carbone, C.T. Laurencin, Prog. Polym. Sci. (2014). doi:10.1016/j.progpolymsci.2014.12.001
15. A.R. Unnithan, R.S. Arathyram, C.H.S. Kim, in *Nanotechnology Applications for Tissue Engineering*, Chap. 3 Electrospinning of Polymers for Tissue Engineering, (Elsevier Mosby, St. Louis, MO, 2015) pp. 45–55
16. M. Spasova, O. Stoilova, I. Manolova, I. Rashkov, J. Bioact. Compat. Polym. **26**, 48 (2011)
17. S.J. Hollister, R.D. Maddox, J.M. Taboas, Biomaterials **23**, 4095 (2002)
18. X. Qi, Z. Mou, J. Zhang, Z. Zhang, J. Biomed. Mater. Res. **102**, 366 (2014)
19. S.H. Wua, X. Liu, W. Kelvin, K. Yeung, Mater. Sci. Eng. R **80**, 1 (2014)
20. S. Ravindran, M. Kotecha, C.C. Huang, A. Ye, P. Pothirajan, Z. Yin, R. Magin, A. George, Biomaterials. (2015). doi:10.1016/j.biomaterials.2015.08.030
21. N. Shadjou, M. Hasanzadeh, Mater. Sci. Eng. C (2015). doi:10.1016/j.msec.2015.05.027.
22. R.C. Younga, G. Terenghia, M. Wiberg, Br. J. Plast. Surg. **55**, 235 (2002)
23. M. Niaounakis, *Biopolymers: Applications and Trends—Processing and Part Fabrication*. (Copyright© 2015 Elsevier B.V), p. 91
24. Niaounakis M (2015) *Biopolymers: Applications and Trends—Definitions of Terms and Types of Biopolymers*. (Copyright© 2015 Elsevier B.V), p. 1
25. H. Hajiali, S. Karbasi et al., J. Mater. Sci. **21**, 2125 (2010)
26. R. Iron, M. Mehdikhani, S. Karbasi, 5th International Congress on Nanoscience & Nanotechnology. ICNN2014
27. N.W. Shi Kam, T.C. Jessop, P.A. Wender, H. Dai, J. Am. Chem. Soc. **126**(22), 6850 (2004)
28. A. Bianco, K. Kostarelos, M. Prato, Chem. Commun. **37**, 10182 (2011)
29. L. Zhuang, T. Scott, W. Kevin Hongjie, Nano Res. **2**(2), 85 (2009)
30. B.S. Harrison, A. Atala, Biomaterials **28**, 44 (2007)
31. A. Bianco, K. Kostarelos, C.D. Partidos, M. Prato, Chem. Commun. **1**, 571 (2005)
32. S. Iijima, Nature **354**, 56 (1991)
33. E.T. Thostenson, Z. Ren, T.W. Chou, Compos. Sci. Technol. **61**, 1899 (2001)
34. P.G. Collins, P. Avouris, Sci. Am. **283**, 62 (2000)
35. H. Zhang, J. Bioact. Compat. Polym. **26**(4), 347 (2011)
36. J.B. Yoo, J.S. Jeong, J.S. Moon, S.Y. Jeong, J.H. Park, J. Phys. Chem. Solids (2006). doi:10.1016/j.tsf.2006.10.058
37. Q. Chen, J.A. Roether, A.R. Boccaccini, in *Topics in Tissue Engineering*, vol 4, ed. by N. Asham makhi, R. Reis, F. Chiellini© 2008
38. H. Wang, Y. Li, Y. Zuo, J. Li, S. Ma, L. Cheng, Biomaterials **28**, 3338 (2007)
39. L. Shor, S. Guceri, X. Wen, M. Gandhi, W. Sun, Biomaterials **28**, 5291 (2007)
40. M.D. Kofron, J.R. Cooper, S.G. Kumbar, C.T. Laurencin, J. Biomed. Mater. Res. **82**, 415 (2007)
41. A. Bagchi, S.R. Meka, B.N. Rao, K. Chatterjee, Nanotechnology **25**(48), 485101 (2014)
42. G.M. Kim, G.H. Michler, P. tschke, Polymer **46**, 7346 (2005)
43. Y. Dror, W. Salalha, R.L. Khalfin, Y. Cohen, A.L. Yarin, E. Zussman, Langmuir **19**, 7012 (2003)
44. Q.U. Song, W. Joseph, Y. Xiao, Chem. Eur. J. **13**(3), 723 (2007)
45. L. Ghasemi Mobarakeh, D. Semnani, M. Morshed, J. Appl. Polym. Sci. **106**, 2536 (2007)
46. ISO 1798:2008 Flexible cellular polymeric materials, Determination of tensile strength and elongation at break. Document published on: 2008-02-01. http://www.iso.org/iso/catalogue_detail.htm?csnumber=41059.
47. S.M. Gubanski, A.E. mastos, IEEE Trans. Power Delivery **5**(3), 1527 (1990)
48. J.M. Deitzel, J. Kleinmeyer, D. Harris, N.C. Beck Tan, Polymer **42**, 261 (2001)
49. M. Naebe, T. Lin, X. Wang, in *Nanofibers*, ed by A. Kumar (InTech, Rijeka, Croatia, 2010), p. 309
50. E.D. Boland, D. Branch, P. Catherine, G. David, E. Gary, L. Gary, Acta Biomater. **1**, 115 (2005)
51. C. Ayres, G.L. Bowlin, S.C. Henderson, L. Taylor, J. Shultz, J. Alexander, T.A. Telemeco, D.G. Simpson, Biomaterials **27**(32), 5524 (2006)
52. J. Stephen, W. William, J. Roy. Soc. Interface **2**, 309 (2005)
53. M.D. Landete-Ruiz, J.A. Martínez-Díez, M.A. Rodriguez-Perez, J.A. De Saja, J.M. Martin-Martínez, J. Adhes. Sci. Technol. **16**, 1073 (2002)
54. J. Amit, Braz. Arch. Biol. Technol (2016). doi:10.1590/1678-4324-2016150644